Remote sensing of avalanches in northern Norway using Synthetic Aperture Radar

Eirik Malnes [(1)], Markus Eckerstorfer[(1)], Yngvar Larsen[(1)],
Regula Frauenfelder[(2)], Árni Jónsson[(2)], Christian Jaedicke[(2)] and Stian A. Solbø[(1)]

[1] Northern research Institute (Norut), Tromsø, Norway
[2] Norwegian Geotechnical Institute (NGI), Oslo, Norway

ABSTRACT: We present results from using synthetic aperture radar data (SAR) to analyse three avalanches in the county of Troms in northern Norway during the late snow season 2013. During a persistent polar low pressure activity at the end of March and the beginning of April 2013, inducing high precipitation rates in combination with high wind speeds, an extensive avalanche cycle took place in that area. Several avalanches released naturally causing fatalities, road closures and community evacuations. The main goal of our study was to investigate whether high resolution SAR could be used for detecting avalanche debris in the run-out zones. For validation purposes we used, among others, a high resolution camera operated on an Unmanned Airborne Vehicle (UAV) to acquire very accurate ortho-photos of the avalanches. The UAV-maps were of unprecedented resolution (~5 cm).

The result of the analysis of the high resolution Radarsat-2 image showed that avalanches could be identified visually due to the high contrast between low radar backscatter from unperturbed snow and high backscatter (caused by increased surface roughness/snow mass) of the avalanche debris in the avalanche run-out zones. In order to assess the accuracy, the avalanche delineations were compared with results from UAV photos and photographs taken during helicopter reconnaissance flights right after the events. In two of three cases, a good correspondence was found between SAR delineated avalanches and outlines derived from optical data.

KEYWORDS: Avalanche detection, Remote sensing, Synthetic Aperture Radar, UAV.

1 INTRODUCTION

Snow avalanches occur frequently in the mountainous areas of northern Norway, which are characterized by a high-relief, alpine topography. This study investigates the use of radar and optical remote sensing sensors to detect and investigate large avalanches. We present results from three avalanches that released in Troms county (see Fig. 1) during intensive polar-low activity in late March and beginning of April 2013. A combination of high wind speeds and snowfall led to an avalanche cycle with extended periods where the issued avalanche danger level was at level 4 (varsom.no). The situation led to several accidents of which three of them caused a total of 5 fatalities. Numerous roads were closed for shorter or longer periods and inhabitants from several local communities had to be evacuated.

Satellite remote sensing frequently covering large areas could potentially be a valuable technique for monitoring avalanches. Satellite data can be used both for detecting snow water equivalent (Rott et al., 2010) and other snow parameters during winter, such as the presence of wet snow (Malnes et al., 2005), snow surface characteristics (Solberg et al., 2009) and snow temperature (Zhou et al., 2008). The potential to use satellite imagery for avalanche danger assessment and forecasting has, however, not yet been well demonstrated, mainly due to lacking capabilities of current satellite sensors (high resolution, frequent coverage, appropriate radar frequencies and sensitivities). Future sensors are expected to yield better capabilities. Additionally, there is also a potential to map the extent of released avalanches using satellites. Lato et al. (2012) showed how very high resolution optical imagery can be used to detect and exactly delineate the extent of released avalanches. However, the study also revealed that detection methods purely relying on optical sensors have limitations during elongated periods with cloud cover. Frequent cloud cover and poor light conditions (the latter typical for high latitude winters) may prohibit detection. In addition, costly satellite data is a major obstacle for the operationalization of optical detection of avalanches.

The here presented study has its main focus on using Synthetic Aperture Radar (SAR) for the detection of avalanches. SAR can be used independent of light and cloud conditions. Wiesmann et al. (2001) demonstrated in an early test case that avalanche deposits can be depicted by SAR backscatter information in ERS1/2 data.

Corresponding author address:
Eirik Malnes, Norut, Tromsø, Norway;
tel: +47 917 58 213; fax: +47 776 29001;
email: eirik@norut.no

Current SAR sensors such as Radarsat-2 (RS-2), TerraSAR-X and Cosmo-Skymed have high-resolution modes that allow imaging down to 2-3 meter spatial resolution. In the current project, funded by the ESA PRODEX programme, we wanted to explore which SAR modes can be best used for the detection of avalanche debris.

2 METHODS AND DATA

2.1 Avalanche and meteorological data

The avalanche activity and the snowpack data was acquired from the website regObs.no, the meteorological data for the stations Troms was acquired from the website eklima.no. Additionally, an official avalanche accident report, issued by the Norwegian Geotechnical Institute (NGI) was used (Brattlien, 2013).

2.2 SAR Data

We used images from Radarsat-2 as a main source of data in this study. Based on the reported avalanches, two RS-2 images with high resolution were ordered for three sites in Norway (Fig. 1). The image over Senja, covering the avalanches in Tromdalen was acquired on April 5, ten days after a severe avalanche accident. This image also covers the avalanche in Steinfjord which released on April 2. An image covering the Kattfjordeidet avalanche was acquired on April 9, five days after the incident.

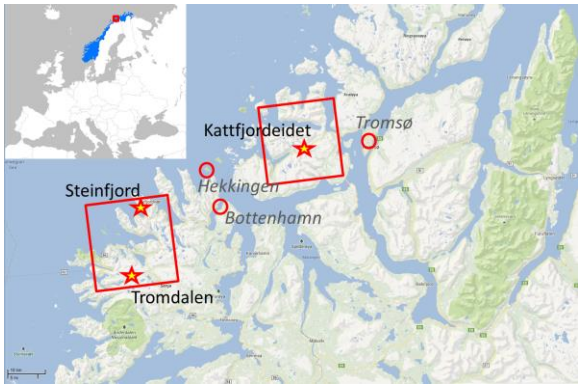

Figure 1. Map over the Troms region in northern-Norway where avalanches were observed with RS-2. Stars indicate the locations of the three avalanches. Red circles show the locations of the closest meteorological stations. Upper left inlet: Location of Troms county.

Both SAR images were acquired in Ultrafine mode with a nominal spatial resolution given as 3 meter. The images were carefully selected in order to avoid radar artefacts such as layover and radar shadow in the regions of interest.

2.3 Supporting datasets

In addition to the two RS-2 images, we also acquired airborne optical validation data for the Steinfjord and Kattfjordeidet sites. In Steinfjord we had access to photos from a helicopter reconnaissance flight carried out by NGI staff on April 3, the day after the avalanche event, whereas the Kattfjordeidet site was mapped using Norut's UAV camera in a separate campaign on April 8, four days after the incident. We also used data from three meteorological stations in the area (Fig. 1).
In addition to this ancillary data we also have a coarser resolution RS-2 SCNA mode (50 m) data set from March 31, 2013 covering all 3 sites. However, due to the coarse image resolution it was not possible to identify avalanches directly in this dataset.

2.4 Image analysis

Prior to the analyses, the SAR images were geocoded to a cartographic projection (UTM zone 33N, WGS-84) using a high resolution digital elevation model (DEM) (20 m horizontal resolution). Based on the visual interpretation of SAR backscatter imagery, we could then draw the avalanche debris outlines, and using GIS allows us to compare these manually derived results with avalanche outlines derived from e.g., optical imagery, UAV imagery or delineations based on information from oblique photographs taken during reconnaissance flights.

3 RESULTS

3.1 Avalanche, snow and meteorological data

Case 1:
The fatal slab avalanches in Tromdalen, Senja released on March 26, 2013. The actions leading to the accident remain unclear, but evidence showed that the first two drivers of a party of three snowmobile drivers were buried by a first release while the third one was killed by a subsequent avalanche. Meteorological conditions prior to the avalanches show air temperatures above 0°C, high wind speeds of up to 16 m/s and a total of 24 mm snow water equivalent of precipitation (Figure 2). The avalanches were most likely soft slab avalanches that released due to natural additional loading onto a thin weak layer of facets found above and between two ice crusts that formed in the end of February. This facet-icecrust sandwich was found in large parts of the Tromsø area and was responsible for other fatal accidents that spring as well (Brattlien, 2013).

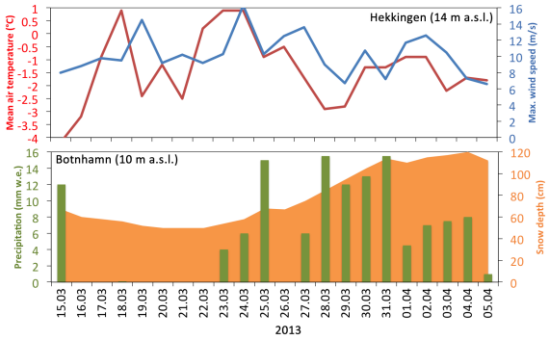

Figure 2. Meteorological data from the two meteorological stations Hekkingen and Bottenhamn, both approximately 30 km northeast of the avalanches in Tromdalen. Data from www.eklima.no.

We do not have an accurate delineation of the avalanches. There exists, however, a well-documented accident report for the site (Brattlien, 2013) providing information about the avalanches. Figure 3 shows the RS-2 backscatter image with overlaid information taken from that report. The results are not easy to interpret. The site is located in a narrow valley surrounded by steep slopes resulting in backscatter from a variety of incidence angles and aspects.

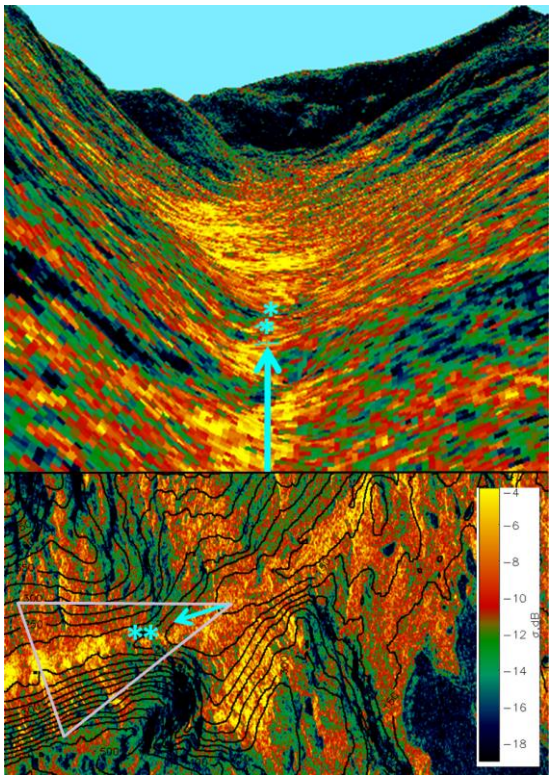

Figure 3. Top: 3D-view westwards into Tromdalen (RS-2 backscatter draped on digital terrain model). Bottom: RS-2 image from Tromdalen with height contours. Asterisks mark the positions where the avalanche victims were found. Arrows and triangle indicate perspective of 3D-view.

Still, we can observe high backscatter (in yellow) in almost the entire valley ground were a lot of avalanche debris became located after extensive artificial triggering during the recovery mission.

Case 2:
On April 2, 2013 a slab avalanche released in Steinfjord, Senja, resulting in the closure of the county road Fv862 connecting local settlements in the area. This avalanche was examined by NGI under a helicopter reconnaissance flight on April 3, and was also captured by the same RS-2 image from April 5 as was used for Case 1.

Meteorological conditions prior and during the avalanche release as well as snow conditions favouring the release were similar to the ones described for Case 1 (Tromdalen).

Figure 4 illustrates the Steinfjord case with a photograph from the site taken from helicopter, and with the classified RS-2 image.

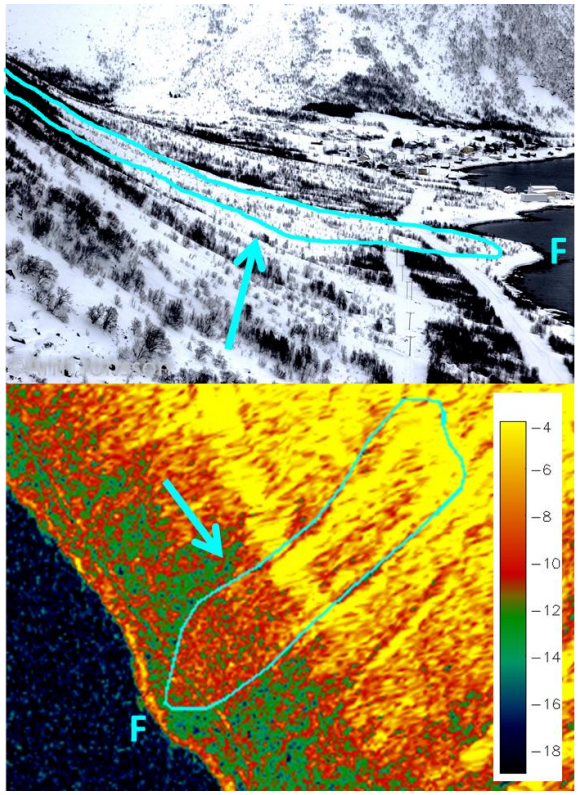

Figure 4. Top: Steinfjord avalanche as captured from helicopter (Image source: Á. Jónsson, NGI). Bottom: RS-2 backscatter image from Steinfjord. Light blue lines: Manual avalanche delineation based on the information from a grayscale backscatter image and reconnaissance flight photographs. Avalanche front is marked with an F. Image perspective from helicopter is marked with arrows.

Case 3:
On March 30, several natural slab avalanches released in the valley Kattfjordeidet, on the island Kvaløya, just west of Tromsø. Meteorological conditions leading to these events exhibited severe polar low activity with over 35 mm water equivalent of precipitation within a week prior to the avalanche (Figure 5). The result was, among others, an avalanche with a crown line of about 900 m, and a debris pile burying the county road Fv862 on over one kilometre length. This road was closed for 14 days before it was cleared and could be reopened.

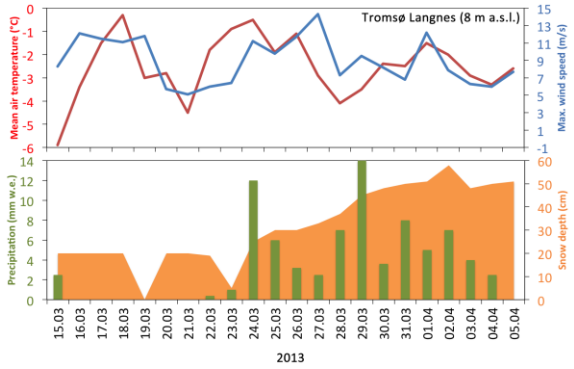

Figure 5. Meteorological data from Tromsø Langnes, approximately 20 km east of the avalanche in Kattfjordeidet.Data from the website www.eklima.no.

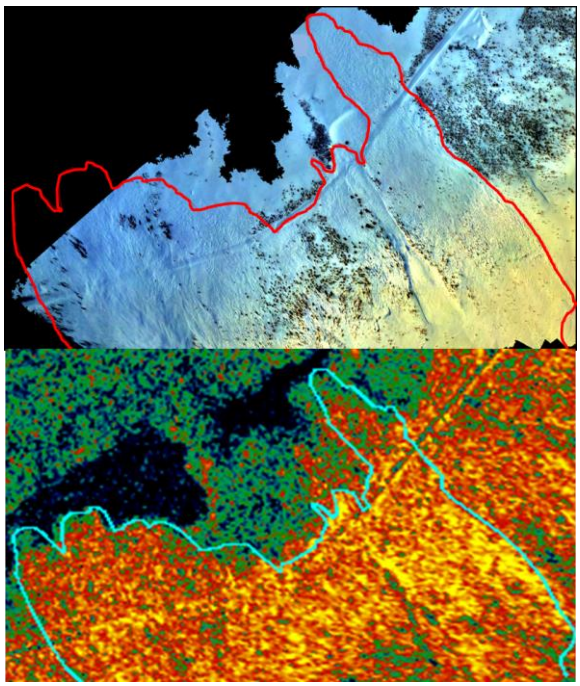

Figure 6. Top: UAV camera image from Kattfjordeidet (black areas are masked due to poor image quality). Bottom: RS-2 backscatter image from Kattfjordeidet. Red/cyan lines: Manual avalanche delineation based on the information from a grayscale backscatter image and reconnaissance flight photographs.

Figure 6 shows the RS-2 backscatter image and UAV imagery with overlaid avalanche outlines, manually delineated based on the information from a grayscale backscatter image and reconnaissance flight photographs.

4 DISCUSSION

As shown in section 3, we note in all three images a generally higher radar backscatter in the avalanche areas than in the surrounding areas with approximately the same slope. Table 1 summarize the backscatter average values and standard deviations within the avalanche areas and in the surrounding areas.

Table 1.Average backscatter values for the three examined sites.

	$\langle\sigma\rangle^t$,inside avalanche (dB)	$\langle\sigma^t\rangle$, outside avalanche (dB)	Contrast (dB)
Tromdalen*	-8.8 ± 2.5	-10.6± 2.8	1.8
Steinfjord	-9.8 ± 2.1	-12.1±2.4	2.3
Kattfjordeid.	-4.9± 2.5	-6.4±2.4	1.5

*) Delineation is uncertain in this area

From Table 1 it can be seen that the contrast in backscatter between the avalanche zones and the surrounding areas with similar hill slope is of the order of 2 decibel (dB). At the same time, the standard deviations in backscatter are of the order 2.5 dB. Although a trained eye can see such differences in backscatter between avalanches and unperturbed slopes relatively easy, it is not strait forward to design an automatical segmentation algorithm for classification of avalanches. The radiometric resolution (related to the standard deviation in backscatter) could to some degree be improved with higher resolution data from, e.g., spotlight mode, or with the same dataset using advanced SAR speckle filtering techniques. A few simple filters were investigated (median-filter) without any visible improvements.

In Case 2 and 3 we can clearly delineate the avalanche paths and confirm these with airborne optical data sets. In Case 1 (Tromdalen) the classification of avalanche tracks is not strait forward. In Fig 3 we observe areas with high backscatter in the valley consistent with where we can expect snow deposits, but the area where the avalanche victims were found did not have significant high backscatter, although snow depths of 6-8 m were reported. The fact that we do not have aerial photos over the area, and that many avalanches were released over an extended period of two weeks with large amount of precipitation makes the interpretation even more challenging.

3.2 Scattering mechanism

As shown in, e.g., Rott et al. (2010) the total scattering from dry snow (σ^T) is a combination of scattering from the ground (σ^g), from the snow volume (σ^V) and for the snow surfaces (σ^{SS}), indicated in equation (1):

$$\sigma^T = \sigma^g + \sigma^v + \sigma^{ss} \quad (1)$$

Usually the contribution from snow volume and snow surface is negligible for dry snow when we apply C-band frequencies (5.6 GHz), but in at least Case 2 and 3 it is evident that a relatively strong scattering mechanism is present. A combination of increased volume scattering due to larger amounts of snow in the lower parts of the avalanche tracks and increased surface scatter due to increased surface roughness could be the reasons. Further analysis and electromagnetic modelling of the scattering effects should be performed to obtain a deeper understanding of the relative importance of these factors.

In this paper we have compared backscatter from avalanche debris with backscatter from surrounding areas with similar slope since backscatter from the ground is strongly dependent of local incidence angles. Differences in ground backscatter caused by other factors, such as rocky debris or different vegetation in avalanche areas and surrounding areas, will have to be ruled out by acquiring identical SAR images under snow free conditions. Change detection analysis will reveal if some of the noticed backscatter increase can be attributed to, for example, rocky terrain.

4 CONCLUSION

This paper explored whether high-resolution C-band Synthetic Aperture Radar data (3 m or better) can be used to map avalanche debris on steep slopes in Norwegian coastal areas. In two of three cases, we could clearly identify avalanches and were able to confirm our findings with optical airborne datasets. The avalanches were identified based on backscatter contrast with respect to surrounding areas with similar slopes.

High resolution C-band SAR could potentially be used as an efficient tool for avalanche mapping, since many of the problems related to cloudiness in optical data is avoided. Depending on favourable image geometry, the lead time between a reported avalanche and image acquisition can also be reduced to 2-5 days, although rush programming of SAR is quite costly. This lead time seems acceptable based on the results in the paper. Daily operational monitoring, e.g., using Sentinel-1, also allowing detection of not-reported avalanches, seems currently not feasible due to poorer image resolution, but should be investigated.

5 ACKNOWLEDGEMENTS

This work has been financed by the ESA PRODEX project ASAM ("Towards an automated snow property and avalanche mapping system"), contracts 4000107724/-664/-694/-722.

Radarsat-2 data has been acquired on a quota from the Norwegian Radarsat-2 agreement. We used a digital elevation model from the Norwegian Mapping Authority (Statens Kartverk).

The reconnaissance flights have been carried out within NGIs commercial services for, among others, the Norwegian emergency services. The UAV acquisition was carried out and funded by Norut. The UAV-pilots A. Tøllefsen and K.S. Johansen are also acknowledged.

6 REFERENCES

Brattlien K., 2013, Skredulykke Tromdalen Senja, Tirsdag 26.03.2013 (in Norwegian),www.snoskred.no

Eklima, 2013, www.eklima.no .

Lato, M., Frauenfelder, R., Bühler, Y., 2012, Automated detection of snow avalanche deposits: segmentation and classification of optical remote sensing imagery. Nat. Haz. And Earth. Syst. Sci., 12, 2893–2906, 2012. doi:10.5194/nhess-12-2893-2012.

Malnes E. , Storvold R., Lauknes I., Solbø S., Solberg R., Amlien J. and Koren H., 2005, Multi-sensor monitoring of snow parameters in Nordic mountainous areas", Proceedings to IGARSS-05, Seoul, South Korea, 25-29 July 2005.

Regobs, 2013, http://www.regobs.no

Rott H., Yueh S., Cline D.W., Duguay C., Essery R., Haas C., Hélière F., Kern M., Macelloni G., Malnes E., Nagler T., Pulliainen J., Rebhan H., Thompson A., 2010, Cold Regions Hydrology High-resolution Observatory for Snow and Cold Land Processes", IEEE Transactions on geoscience and remote sensing, 99, 1-10.

Solberg R., Frauenfelder R., Koren H. and Kronholm K., 2009, Could retrieval of snow layer formation by optical satellite remote sensing help avalanche forecasting? , Presentation of first results, ISSW proceedings Davos 2009

Varsom, 2013. http://www.varsom.no

Wiesmann, A., Wegmüller, U., Honikel, M., Strozzi, T., Werner, C.L. 2001. Potential and methodology of satellite based SAR for hazard mapping. Proceedings of IGARSS 2001, Sydney, Australia, 9 - 13. July 2001. 0-7803-7031-1/01 (C) 2001 IEEE.

Zhou J., Chen Y., Tang Y., 2008, Retrieval of snow surface temperature based on MODIS data, Geospatial Information Science, 11:4, 247-251.